

Supporting Information

**‘Thermal substitution’ for preparing ternary BCN
nanosheets with enhanced and controllable nonlinear optical
performance**

Fukun Ma, Mengxia Wang, Yongliang Shao, Lijuan Wang, Yongzhong
Wu, Zhengping Wang,* and Xiaopeng Hao*

State Key Lab of Crystal Materials, Shandong University, Jinan, 250100,
China

E-mail: zpwang@sdu.edu.cn; xphao@sdu.edu.cn

Table of contents:

S1. AFM image of as-prepared BCN nanosheets

S2. FTIR spectra of as-prepared BCN nanosheets

S3. Transmission spectra of as-prepared BCN nanosheets

S4. Z-scan experimental setup

S5. Passively Q-switched laser performance of BCN nanosheets

S1. AFM image of as-prepared BCN nanosheets

The thickness of the as-obtained BCN nanosheets is measured by AFM, as shown in Figure S1. Each layer presents a thickness of 2–3 nm.

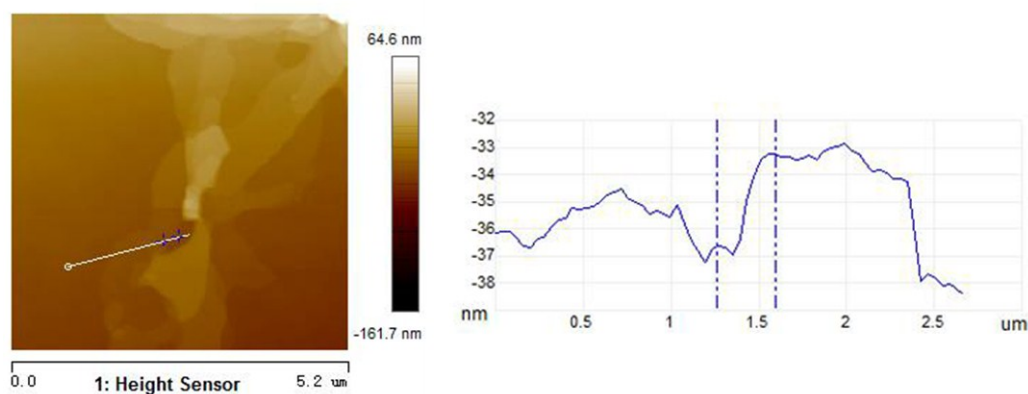


Figure S1. AFM image of the as-obtained BCN nanosheets

S2. FTIR spectra of as-prepared BCN nanosheets

Figure S2 shows the FTIR spectra of the BNNSs and the BCN nanosheets. Two typical sharp absorption peaks of the BNNSs were observed at 1373.3 and 817.8 cm^{-1} (caused by the in-plane B-N stretching vibration and the B-N-B out-of-plane bending vibration respectively). There are new peaks in the structure of BCN nanosheets, which suggest the C=N bonds in the structure.¹

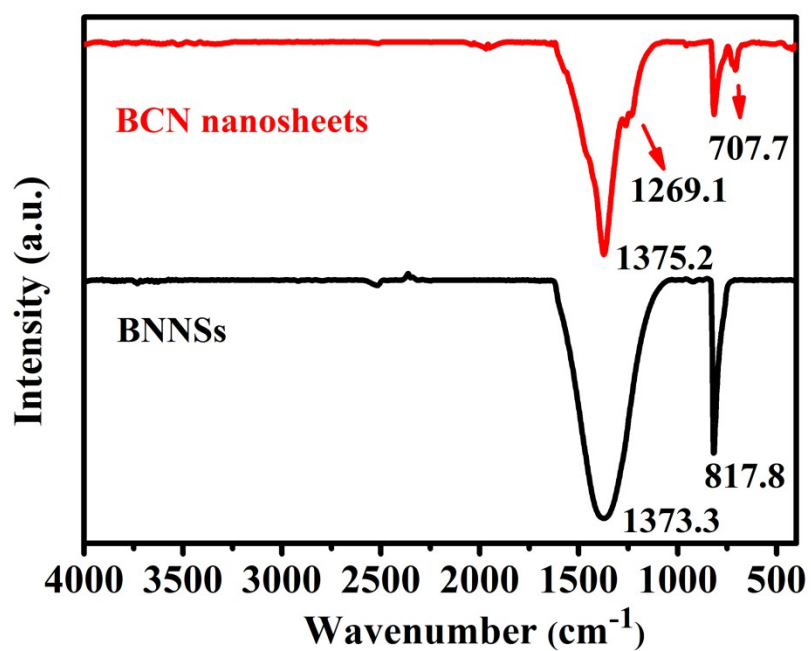


Figure S2. FTIR spectra of the as-obtained BCN nanosheets and BNNSs.

S3. Transmission spectra of as-prepared BCN nanosheets

The dispersibility of BCN nanosheets was validated by dispersing the nanosheets in ethanol (Figure S3). The dispersion of our products is very stable, and the dispersion in ethanol has been stable over 180 days. These features make the obtained BCN nanosheets suitable for NOL test.

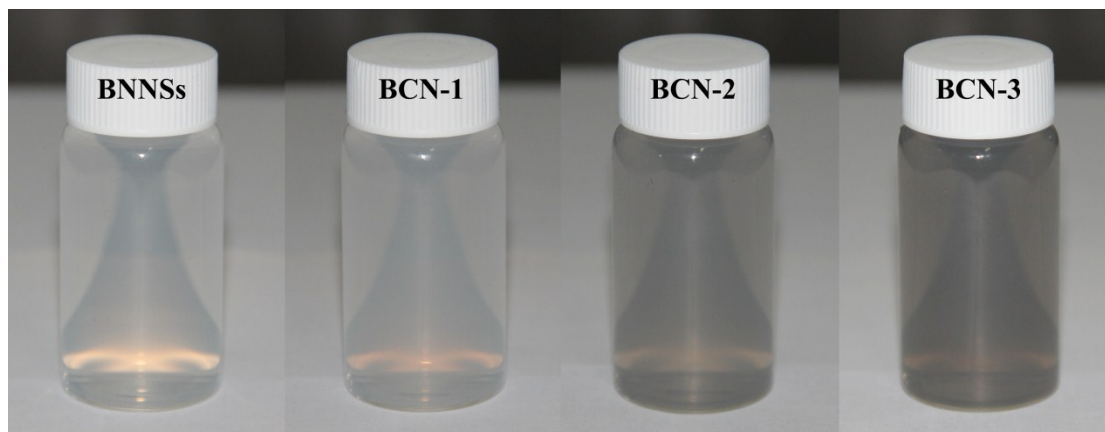


Figure S3. Photograph of BNNSs and BCN nanosheets.

S4. Z-scan experimental setup

The Z-scan technique was used to investigate the nonlinear optics properties of the as-prepared BCN samples. The experimental setup is shown in Figure S4. The laser resource is a dye mode-locked Nd:YAG laser (PY61C-10, Continuum Inc, America), which can operate at the fundamental wavelength of 1064 nm, as well as the second-harmonic-generation (SHG) wavelength of 532 nm. The pulse width is 35 ps or so, and the repetition rate is 10 Hz. The focal length of the convex lens is 30 cm.

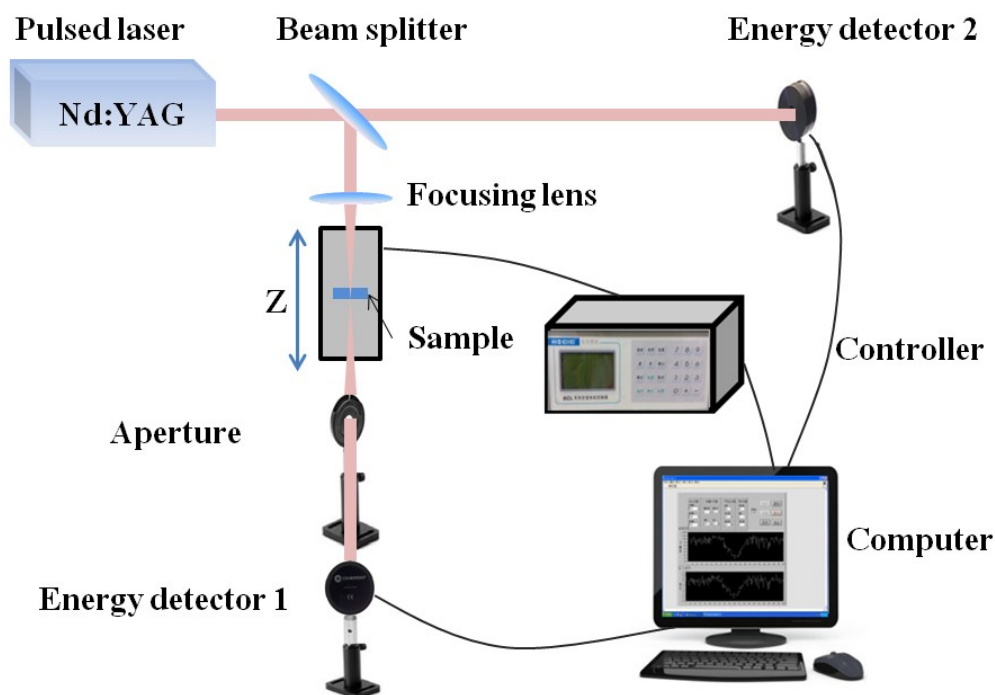


Figure S4. Diagram of the Z-scan experimental setup.

S5. Passively Q-switched laser performance of BCN nanosheets

With a plano-concave laser resonator, we investigated the passively Q-switched laser performance of the BCN-3 nanosheets and the BNNSs. The experimental setup is shown as follow, and the results are shown in Figure S6.

The schematic of the passively Q-switched solid-state lasers is demonstrated in Figure S5. The pump source was a 808 nm fiber-coupled diode laser ($\phi = 100 \mu\text{m}$, N.A. = 0.22). The transfer ratio of the focusing system was 1:1. A 0.8 mm thick Nd:GdVO₄ crystal with a Nd³⁺ doping concentration of 2 at% was used as the laser medium. It was held in a copper block which was cooled by circulating water with fixed temperature of 15 °C. The left end face of the laser crystal which was closed to the pump source was high transmission (HT) coated at 808 nm and high reflection (HR) coated at 1064 nm, to serve as the input mirror M1 of the laser resonator. The other end face of the laser crystal was HT coated at 1064 nm and HR coated at 808 nm, which is favorable for the laser oscillation and the re-absorption of the pump power. The output coupler M2 was a concave mirror (T = 5%, R = 100 mm). The BCN-3 and BNNSs samples were deposited on the different glass plates under the same conditions, which were used as the saturable absorbers (SA) successively. The average output power was measured by a power meter (POWERMAX 500D, Molelectron Inc.). The temporal behaviors of the Q-switched laser were recorded by a digital oscilloscope with 1 GHz bandwidth and 2.5 Gs s⁻¹ sampling rate (DPO7104, Tektronix Inc.).

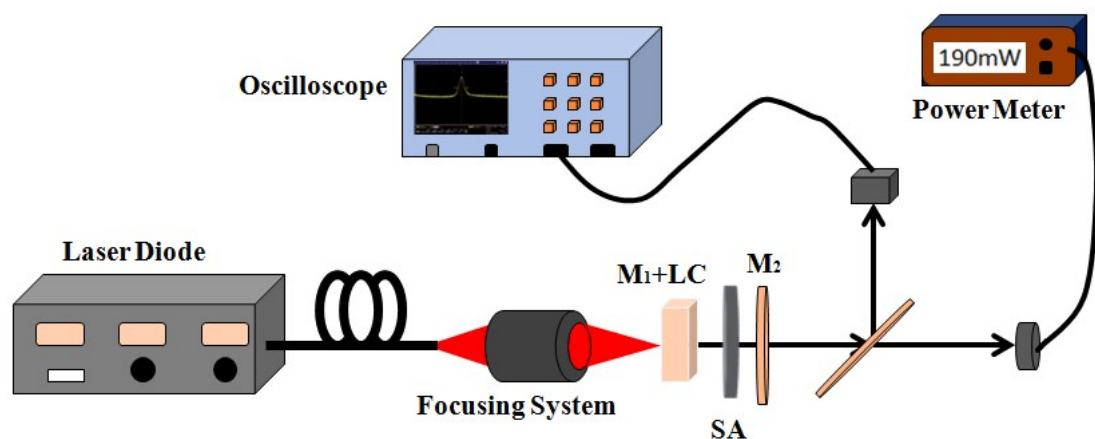


Figure S5. Experimental setup of the passively Q-switched solid-state lasers.

When the saturable absorber (BCN-3 or BNNSs) is removed from the resonator, the 1064 nm continuous-wave (CW) laser output is obtained. The pump threshold is 16 mW, and the maximum CW output power is 190 mW under an incident pump power of 480 mW, corresponding to an optical conversion efficiency of 39.6%, as seen in Figure S6a. The pulse Q-switched properties of the BCN-3 nanosheets and the BNNSs are compared in Figure S6a~e. When the BCN-3 saturable absorber is inserted into the laser cavity, the passively Q-switched operation is achieved when the incident pump power exceeds 124 mW. With the increase of pump power, the average output power, repetition rate, single pulse energy, and peak power also increase, while the pulse width presents a decreasing trend. The maximum average output power of 24 mW is obtained at a pump power of 480 mW, and the optical conversion efficiency is 5%. The highest repetition rate and the shortest pulse width are 537.0 kHz, 121.8 ns, respectively, which are demonstrated Figure S6f. Correspondingly, the largest pulse energy is 0.045 μ J and the highest peak power is 0.367 W. When the BNNSs is used as the saturable absorber, the pump threshold of the passively Q-switched operation is

189 mW, and the maximum average output power is 18 mW which is obtained at a pump power of 850 mW, corresponding to an optical conversion efficiency of 2.1%. At the point of the maximum average output power, the highest repetition rate, the shortest pulse width, the largest pulse energy, and the highest peak power are 730 kHz, 136 ns, 0.025 μ J, 0.184 W, respectively. The corresponding pulse train and pulse profile are shown in Figure S7. Through the comparison of Figure S6f and Figure S7, one can see that the BCN-3 nanosheets have exhibited more stable and uniform Q-switched laser pulse train than the BNNSs. In summary, during the passively Q-switched laser experiments, the BCN-3 nanosheets have presented superior saturable absorption property than the BNNSs, including larger average output power and pulse energy, shorter pulse width, higher peak power, and better pulse stability and uniformity, which is in accordance with the discipline of Figure 4c.

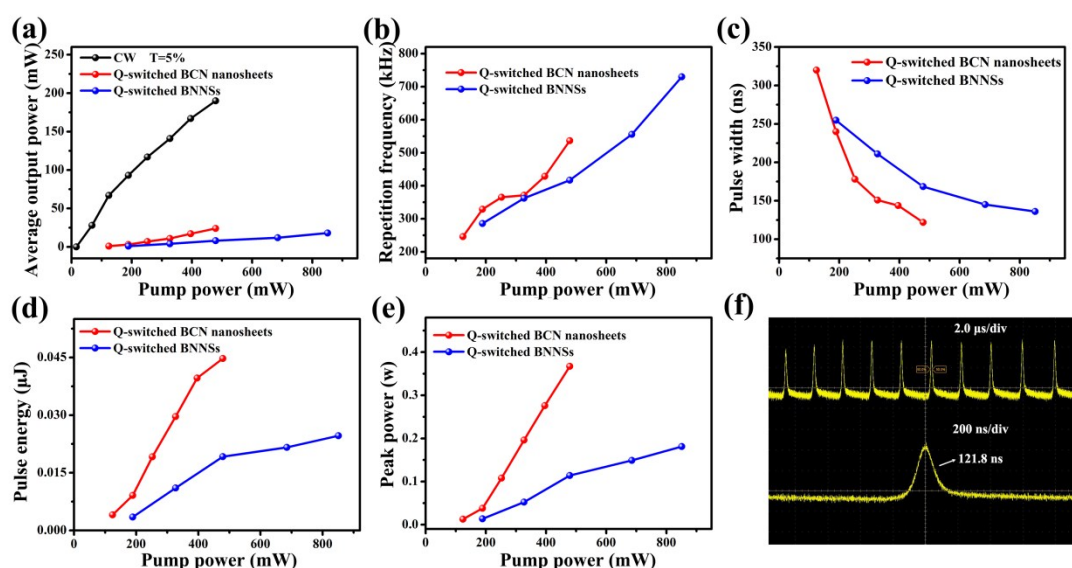


Figure S6. Passively Q-switched laser performance of the BCN-3 nanosheets and the BNNSs. (a) Average output power versus incident pump power. (b) Repetition frequency versus incident pump power. (c) Pulse width versus incident pump power.

(d) Single-pulse energy versus incident pump power. (e) Pulse peak power versus incident pump power. (f) Pulse train with a repetition rate of 537.0 kHz and the corresponding pulse profile with a width of 121.8 ns for the BCN-3 nanosheets.

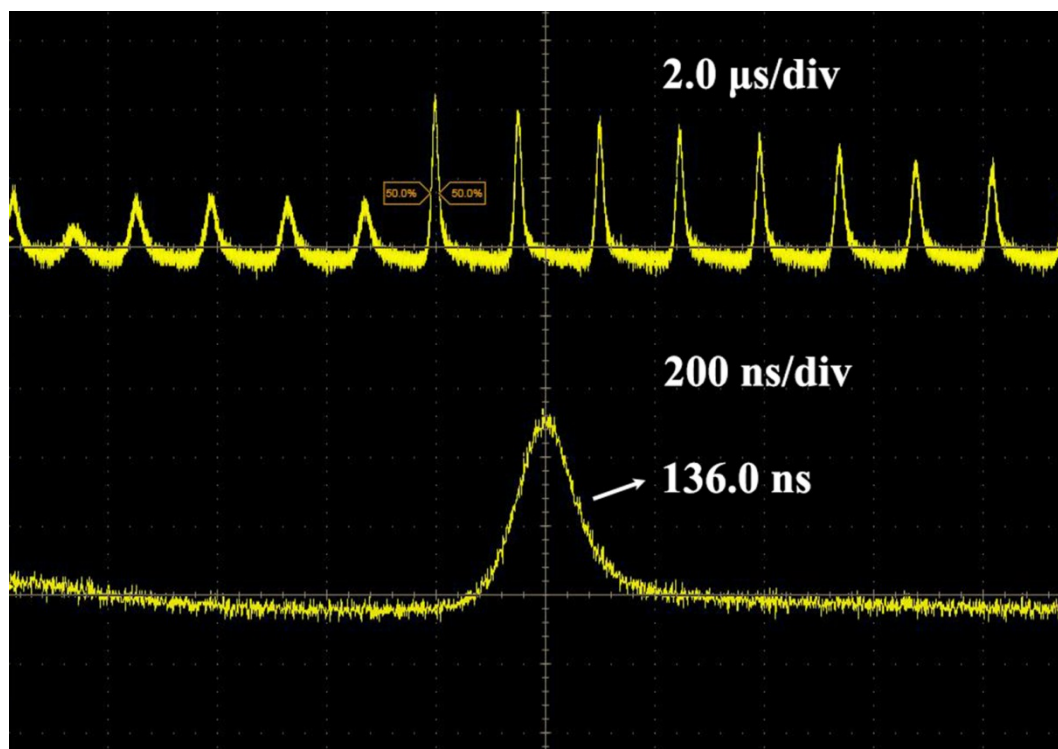


Figure S7. Pulse train with a repetition rate of 730 kHz and the corresponding pulse profile with a width of 136 ns for the BNNSs.

References

- 1 P. Niu, L. Zhang, G. Liu and H.M. Cheng, *Adv. Functional Mater.* 2012, **22**, 4763-4770.